Optimizing Well Trajectories for Enhanced Oil Production in Naturally Fractured Reservoirs: Integrating Particle Swarm Optimization with an Innovative Semi-Analytical Model Framework

Jin Shu[1], Guoqing Han[1]*, Zhenduo Yue[1], Lei Cheng[1], Ya Dong[1], and Xingyuan Liang[1]

[1]China University of Petroleum, Beijing

Summary

Well trajectory optimization is a crucial component in the drilling engineering of naturally fractured reservoirs. The complex heterogeneity and anisotropy of such reservoirs significantly affect the pressure drop distribution within the well and, consequently, the oil well's output, impacting the economic benefits of the well. Therefore, optimizing the well segment trajectory is key to efficient reservoir development. However, traditional well trajectory optimization methods primarily focus on geological structures and drilling engineering costs, often overlooking future production benefits of the oil well. This paper proposes a new method that first establishes a semi-analytical production prediction model capable of describing complex well trajectories. Although the semi-analytical model has unique advantages in well trajectory description, it typically treats the reservoir as a homogeneous entity, which complicates handling complex reservoir characteristics. To overcome this limitation, we combined optimization algorithms and neural networks to construct a framework for addressing reservoir heterogeneity (Semianalytical Model Framework for Unconventional Wells in Heterogeneous Reservoirs, USAMF-HR), enhancing the semi-analytical model's ability to describe reservoir heterogeneity. Building on this framework, we applied the particle swarm optimization (PSO) algorithm and introduced constraints on the rationalization of initial well trajectories, as well as limits on particle movement speed and displacement, with the maximization of net present value (NPV) as the objective function, to optimize well trajectory coordinates. Through specific case analysis, the reasonableness and practicality of this method have been verified. The results show that this method can quickly and effectively plan the optimal well trajectory, significantly increasing productivity while reducing costs.

Introduction

Well trajectory optimization is a key aspect of drilling engineering, with scholars typically studying it from the perspectives of geological conditions, engineering constraints, and economic benefits (Peshkov et al. 2023; Rizkiaputra et al. 2023; Vishnumolakala et al. 2023). By considering factors such as formation stability, wellbore geometry, and cost minimization, optimizing well trajectory design not only enhances drilling efficiency but also reduces operational risks (Li et al. 2024). In addition, the development of optimization algorithms such as PSO and genetic algorithms (GAs) has provided more scientific and effective solutions for well trajectory optimization (Ghadami et al. 2022; Wang et al. 2016; Kasravi et al. 2017). In recent studies, Liu et al. (2022) utilized gradient descent to successfully determine the optimal well location and introduced an innovative and efficient optimization method based on the 3D Dubins curve for the first time in the drilling industry. Concurrently, Chen et al. (2024) considered both geological and engineering factors by incorporating the entire geological profile into traditional design processes. They used artificial intelligence algorithms to mathematically evaluate geological profiles, forming new optimization targets that provide a crucial basis for well trajectory design. Additionally, Singh et al. (2024) explored the design and optimization of well trajectories for sidetracking and deepening wells. They generated well trajectories based on the minimum curvature method and further optimized them using GAs. Pathan et al. (2023) focused on the risk of well trajectory collisions with legacy wells and minimized drilling length as an optimization goal, optimizing the well trajectory using evolutionary algorithms.

However, during the development of naturally fractured reservoirs, the presence of fractures significantly affects the physical properties of the reservoir, such as permeability, porosity, and pore structure, exhibiting marked heterogeneity or anisotropy (Bazalgette et al. 2022; Han et al. 2019). Under such circumstances, different well trajectory segments within the reservoir can lead to significant variations in oilwell productivity (Dou et al. 2022). A well-designed well trajectory can effectively use natural fractures as high-efficiency flow channels (Gu et al. 2022; Grechishnikova 2016; Al-Aruri et al. 2022), thereby enhancing the productivity of the oil well. Therefore, when considering the long-term production benefits of the oil field, the productivity factor becomes particularly important in well trajectory design (Wan et al. 2023; Yu et al. 2023). This method ensures that optimization not only addresses engineering and economic constraints but also maximizes potential output by fully leveraging the intrinsic characteristics of the reservoir (Lyngra et al. 2015; Wu and Olson 2016).

The core of calculating oilwell productivity involves establishing a reservoir seepage model, commonly solved using analytical, semi-analytical, and numerical methods, thus categorized into analytical, semi-analytical, and numerical models. For unconventional wells, the complex nature of completion segments makes it difficult for analytical models to accurately simulate well trajectories. Moreover, the pressure drop within the completion segment significantly influences the reservoir's flow field and should not be overlooked. In such cases, coupling between the wellbore and the reservoir often needs to be considered. Numerical models tend to discretize the reservoir, but the temporal and spatial scale differences between the reservoir and the wellbore make coupling challenging. Semi-analytical models

*Corresponding author; email: guoqing@cup.edu.cn

Original SPE manuscript received for review 22 July 2024. Revised manuscript received for review 14 October 2024. Paper (SPE 223939) peer approved 28 October 2024.

use source functions to discretize the source and sink terms instead of the seepage medium, allowing for precise descriptions of these terms and overcoming the issue of matching temporal and spatial scales during wellbore and reservoir coupling. This has led to the widespread application of semi-analytical models in scenarios involving complex sources and sinks, such as unconventional wells and fractured horizontal wells. For instance, Cui et al. (2022) developed a semi-analytical model for shale gas development in multilevel well pads, focusing on nonuniform fractures and interwell interactions to elucidate complex underground fluid dynamics through type curves. Jiang et al. (2020) established a semi-analytical theoretical model that addresses transient pressure analysis in fractured vertical wells with complex fracture networks, incorporating stress sensitivity. Wei et al. (2020) also created a semi-analytical finite conductivity wellbore model to address pressure drops in multilateral horizontal wells, effectively simulating 3D flows between the wellbore and reservoir to enhance analysis of transient pressure responses in various multilateral horizontal well configurations. However, the nondiscretization nature of seepage media in semi-analytical models means they cannot describe heterogeneous reservoirs like naturally fractured reservoirs. Therefore, it is necessary to optimize the semi-analytical methods.

Addressing the optimization of well trajectories in naturally fractured reservoirs, this paper proposes an innovative method for well trajectory optimization. Initially, we developed a new framework named USAMF-HR, designed to predict production capacity for any well trajectory within naturally fractured reservoirs. To accommodate this framework, we designed a PSO algorithm to find the optimal well trajectory. In the USAMF-HR semi-analytical production prediction model, the wellbore is precisely discretized to describe various well trajectories. Furthermore, by incorporating skin factors along with reservoir numerical simulation, optimization algorithms, and neural network technology, this framework comprehensively describes the reservoir's heterogeneity, significantly enhancing the accuracy and effectiveness of predictions. Through hydroelectric simulation experiments and numerical simulations, we have verified the accuracy and reliability of USAMF-HR under both homogeneous and heterogeneous reservoir conditions. In the PSO phase, the study uses the NPV of the well as the optimization goal, introducing boundary constraints and trajectory rationality constraints as conditions to ensure the reasonableness of the optimization results and to enhance the algorithm's convergence speed. The research findings demonstrate that the well trajectory optimization method proposed in this paper not only effectively enhances the economic benefits of oil wells but also significantly advances the technical level of fractured reservoir development and understanding of the role of fracture networks in reservoir development.

Methodology

In the development of naturally fractured reservoirs, traditional vertical or horizontal wells often fail to adapt to the complex heterogeneity of the reservoirs, making well trajectory optimization crucial for enhancing extraction efficiency. To address this challenge, we propose an optimization problem aimed at designing the optimal well trajectory to maximize the NPV of naturally fractured reservoirs. The objective function considers oil price fluctuations, engineering costs, and other economic factors, reflecting the economic viability of the project. To this end, the wellbore is discretized, and the coordinates and angular combinations of different discrete units are used as decision variables to describe the well trajectory. Constraints are set on the angles between adjacent discrete units and boundary conditions to ensure a rational geometric layout of the well trajectory.

To effectively support this optimization task, we developed the USAMF-HR framework, which integrates the precision of semi-analytical models in describing unconventional well trajectories with the detailed capability of numerical simulations in handling complex reservoir features, achieving accurate production prediction for unconventional wells under heterogeneous reservoir conditions. This framework provides precise predictions of unconventional well productivity, supporting the optimal selection of decision variables. By using this approach, we ensure technical feasibility while optimizing well trajectory design to maximize the efficiency of oil and gas extraction.

USAMF-HR. First, the wellbore is discretized into multiple segments, which allows us to approximate the description of any well trajectory. At the same time, we consider the coupling effects between reservoir permeation and wellbore flow (Apisaksirikul and Blasingame 2016; Clarkson et al. 2014; Zhu and Zhao 2016), as illustrated in the wellbore section diagram shown in **Fig. 1**.

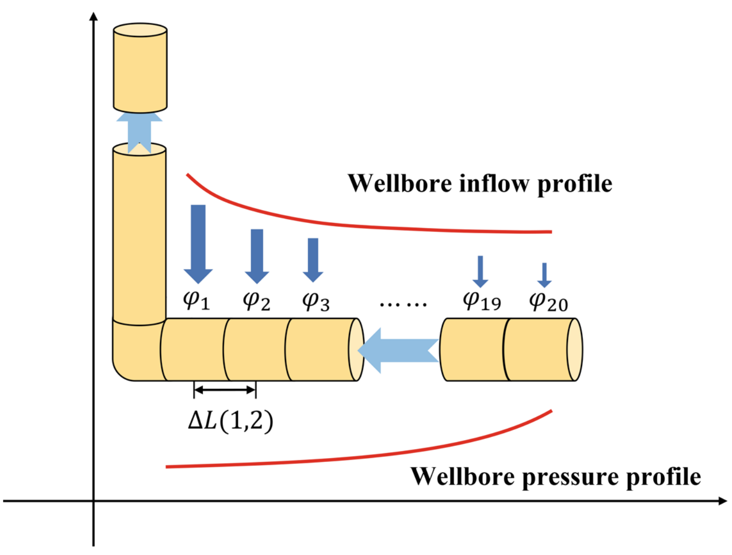

Fig. 1—Wellbore section diagram.

Dimensionless variables are defined:

$$\begin{cases} t_D = \dfrac{kt}{\phi \mu c_t x_e^2} \\ q_D = \dfrac{qB\mu}{kx_e \varphi_i} \\ \varphi_D = \dfrac{\varphi_i - \varphi}{\varphi_i} \end{cases}, \tag{1}$$

where t_D is the dimensionless time, k is the permeability (md), t is the time (seconds), ϕ is the porosity (fraction), μ is the viscosity (Pa·s), c_t is the compressibility (Pa^{-1}), x_e is the length of reservoir boundary, q_D is the dimensionless production rate of well, q is the production rate (m^3/d), B is the volume factor (m^3/m^3), φ_i is the initial reservoir potential (J/kg), φ_D is the dimensionless potential, φ is the potential (J/kg), and i is the index number of any discrete wellbore element.

In the reservoir, each discrete element is considered as an independent line source, adhering to the superposition principle. For a homogeneously anisotropic box-shaped reservoir, the adiabatic flow of fluids can be described by the corresponding partial differential equation (Eq. 2), including the effects of gravity, which are considered in terms of potential.

$$k_x \frac{\partial^2 \varphi}{\partial x^2} + k_y \frac{\partial^2 \varphi}{\partial y^2} + k_z \frac{\partial^2 \varphi}{\partial z^2} = \phi \mu c_t \frac{\partial \varphi}{\partial t}, \tag{2}$$

where $\varphi = p + \rho g h$, φ is the potential (J/kg), p is the pressure (Pa), ϕ is the porosity (fraction), μ is the viscosity (Pa·s), and c_t is the compressibility (Pa^{-1}).

We use the instantaneous point source method to calculate the continuous line source solution in a box-shaped reservoir (Mienzan and Asumadu 2020; Wang et al. 2022; Cao et al. 2022). Based on this solution, the potential difference of any line source can be obtained. According to the principle of potential superposition, the potential difference at the midpoint of each segment in the wellbore can be determined (Eq. 3).

$$\varphi_{wD}\left(i_s\right) = \frac{\varphi_i - \varphi_w\left(i_s\right)}{\varphi_i} = \sum_{j_s=1}^{20} q_{ID}(j_s)\varphi_D(j_s)[M(i_s)], \tag{3}$$

where $\varphi_{wD}\left(i_s\right)$ is the dimensionless potential difference at point M, $\varphi_w\left(i_s\right)$ is the potential at point of the segment numbered as i_s (J/kg), $q_{ID}\left(J_s\right)$ is the dimensionless inflow/outflow of the segment numbered as i_s, $\varphi_D\left(j_s\right)$ is the dimensionless potential of the segment numbered as i_s, and $M\left(i_s\right)$ is the endpoint of the segment numbered as i_s.

Describing the heterogeneity of reservoirs has always been a major challenge for semi-analytical models (Zhao 2013). To effectively address the heterogeneity of naturally fractured reservoirs, we developed a new framework called USAMF-HR **(Fig. 2)**. Within this framework, we first introduce skin factors to represent the impact of permeability heterogeneity in the near-wellbore area on flow within the wellbore (see Eq. 4).

$$s = \left(\frac{k}{k_a} - 1\right) \ln \frac{r_a}{r_w}, \tag{4}$$

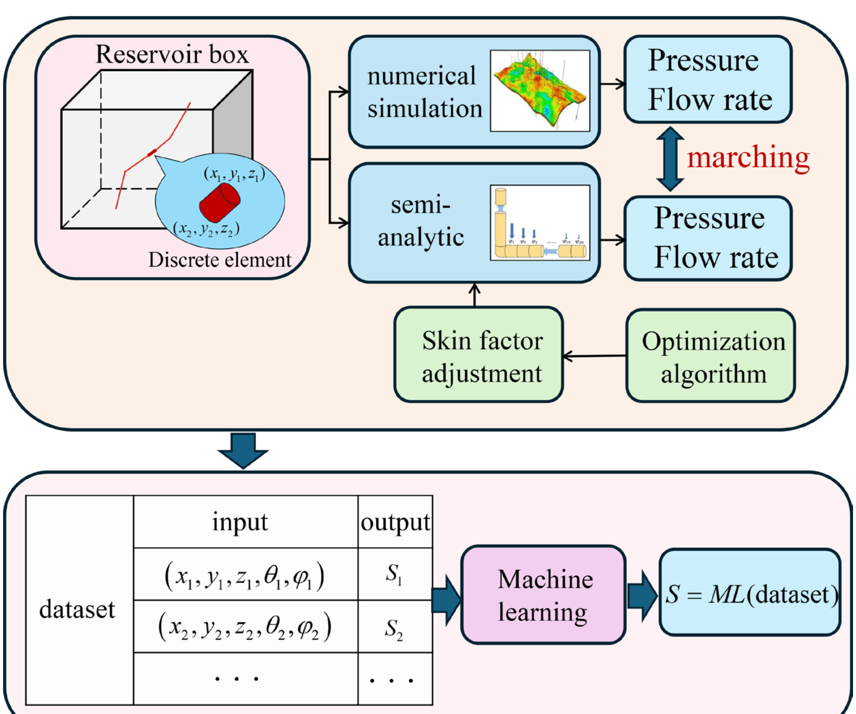

Fig. 2—USAMF-HR.

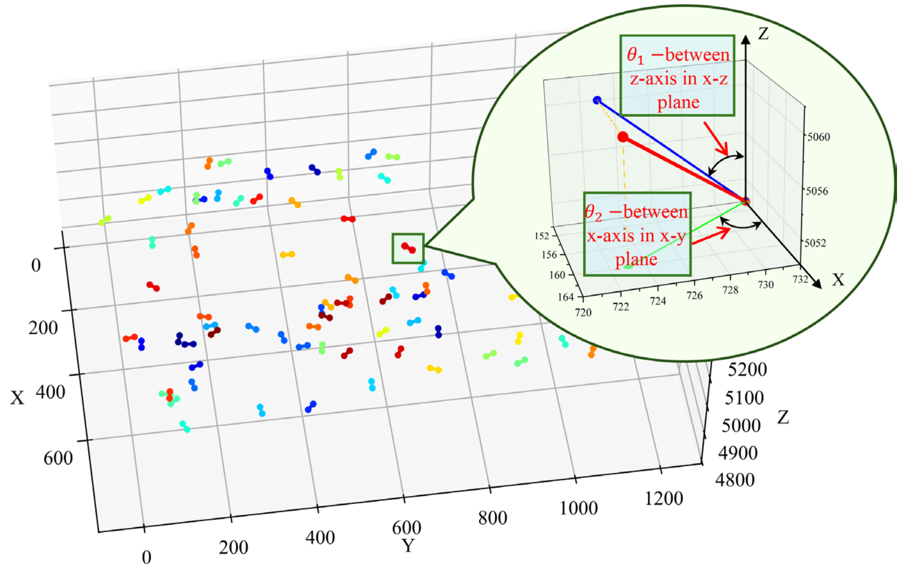

Fig. 3—Well segments generated randomly.

where k is the average permeability of the reservoir, and k_a is the permeability near the wellbore ($r_w < r < r_a$). We assume there are n line sources, where the skin factor of the ith line source is S_i and its potential at the axial distance r_w represents the potential of that well segment. Using the principle of superposition, the potential expression influenced by itself and other segments can be calculated (Eq. 5).

$$\phi_D^w(S_i) = \sum_{n}^{j=1} q_{ID}(S_j)\phi_D\left(M_i, S_j\right), \tag{5}$$

where $\phi_D\left(M_i, S_j\right)$ is the Green's function obtained from the instantaneous point source solution, and $q_{ID}\left(S_j\right)$ is the dimensionless reservoir flow within segments import/export volume.

With known permeability distribution of the reservoir, the production and pressure for each discrete element can be calculated using numerical simulation. By adjusting the skin factors, the production and pressure results from the semi-analytical model are made to approximate those from the numerical simulation, constituting a typical optimization problem. We have chosen the PSO algorithm to quickly find suitable skin factors, although theoretically any effective optimization algorithm could be used for this purpose.

We generate multiple sets of discrete elements randomly, with each element's position defined as follows: The length of the element is fixed, and the spatial coordinates of the first endpoint are randomly set. Then, using the positive directions of the x-axis and z-axis as references, the angles between the x-axis in the x-y plane and the z-axis in the x-z plane are randomly determined as rotation angles. Thus, the position of each discrete element is represented by five-dimensional data comprising the initial point coordinates and two rotation

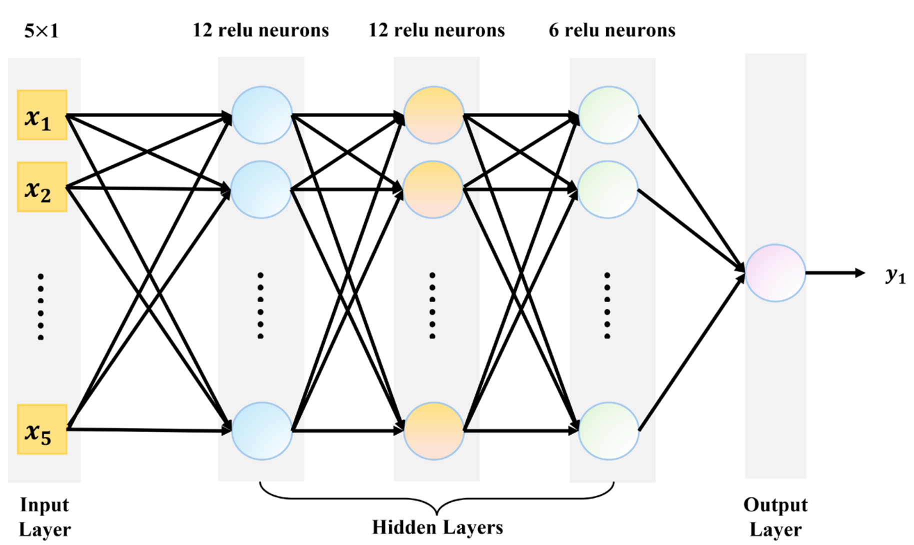

Fig. 4—Neural network model with three fully connected layers.

```
Input  : unit_length, num_samples, Data_trajectory
Output: P_wf_sa, Q_sa

// Step 1:  Preparation
Dataset ← generate_random_samples(num_samples)
Skin_list ← [ ]

// Step 2:  Calculate skin factors using optimization
for sample in Dataset do
    Simulator_Output ← reservoir_simulator(sample)

    // Define the optimization objective function
    def OptimizationObjective(Skin):
        Model_Output ← semi_analytical_model(sample, Skin)
        error ← error_metric(Simulator_Output, Model_Output)
        return error
    Skin_optimal ← PSO(OptimizationObjective)
    Skin_list.append(Skin_optimal)
end

// Step 3:  Augment the dataset and train the neural
   network
Dataset_with_Skin ← append_skin_factors(Dataset, Skin_list)
NeuralNetworkModel ← train_neural_network(Dataset_with_Skin)

// Step 4:  Predict skin factors for the trajectory data
Predicted_Skin_list ← [ ]
for sample in Data_trajectory do
    Predicted_Skin ← NeuralNetworkModel.predict(sample)
    Predicted_Skin_list.append(Predicted_Skin)
end

// Step 5:  Estimate pressure and rate using the
   semi-analytical model
P_wf_sa, Q_sa ← semi_analytical_model(Data_trajectory,
 Predicted_Skin_list)

return P_wf_sa, Q_sa
```

Fig. 5—Pseudocode of the USAMF-HR.

angles. Through this method, the skin factor for each element is determined via the optimization process described above, forming a data set **(Fig. 3)**. Additionally, we have developed a simple neural network model (Ma et al. 2023; Zhen et al. 2024) **(Fig. 4)**, which, after being trained, can predict the skin factor for any discrete element.

Finally, by connecting and combining multiple discrete elements with different skin factors, we can represent the complex well trajectory under the current conditions of the heterogeneous reservoir.

Regarding the flow within the wellbore, we consider only the steady-state flow of a single-phase fluid, as indicated by the dynamics equation (Eq. 6), where the pressure drop in the wellbore is composed of acceleration, friction, and gravity pressure drops. The pressure drop within the wellbore is represented as (Eq. 7).

$$\frac{dp}{dx} = -2\rho q \frac{U}{A} - \tau_w \frac{S}{A} - \rho g \sin\theta, \tag{6}$$

$$\varphi(i_s + 1) = \varphi(i_s) + \Delta p_f\,(i_s; i_s + 1) + \Delta p_a\,(i_s; i_s + 1) + \Delta p_g\,(i_s; i_s + 1), \tag{7}$$

where $\varphi_w\left(i_s\right)$ is the potential at point of the segment numbered as i_s (J/kg), $\Delta p_f\,(i_s; i_s + 1)$ is the difference between the bottomhole flow pressure of the segment numbered as i_s and that of the segment numbered as $i_s + 1$, $\Delta p_a\,(i_s; i_s + 1)$ is the difference between the acceleration pressure drop of the segment numbered as i_s and that of the segment numbered as $i_s + 1$; and $\Delta p_g\,(i_s; i_s + 1)$ is the difference between the gravity pressure drop of the segment numbered as i_s and that of the segment numbered as $i_s + 1$.

$$\Delta p_f\,(i_s; i_s + 1) = \frac{4\tau_w\,(i_s; i_s + 1)}{D}\Delta L\,(i_s; i_s + 1), \tag{8}$$

$$\Delta p_a\,(i_s; i_s + 1) = \frac{2}{A}\rho U q_1 \Delta L\,(i_s; i_s + 1), \tag{9}$$

$$\Delta p_{\mathrm{g}}\left(i_s, i_s + 1\right) = \rho g A \Delta L\left(i_s, i_s + 1\right). \tag{10}$$

In addition, the mass conservation equation is

$$\sum_{i_s=1}^{i_s=20} q_{ID}(i_s) = q_D, \tag{11}$$

where $\tau_w\left(i_s; i_s+1\right)$ is the tangential friction in the wellbore from point i_s to point i_s+1 (N), ρ is the density (kg/m^3) $\Delta L\ (i_s; i_s+1)$ is the distance from point i_s to point i_s+1 (m), and A is the cross-sectional area (m^2).

Finally, by combining the potential difference equation of reservoir permeation, the wellbore flow equation, and the mass conservation equation, we have established a semi-analytical coupled model of the wellbore reservoir. This model can be solved through iterative methods. The overall pseudocode for the USAMF-HR is referenced in **Fig. 5**.

Validation of USAMF-HR. The hydraulic-electric simulation experiment is based on similarity criteria, validating the model's accuracy by comparing the ratios of electric current and production capacity (Yildiz and Deniz 1998). This method's significant advantage lies in its ability to simulate various well trajectories by bending metal wires into different shapes, thereby showcasing the USAMF-HR's capability in precisely describing well trajectories. To demonstrate this diversity, we have designed several types of well trajectories **(Fig. 6)**, each intended to highlight a specific capability of the model:

- Simple horizontal wells, representing the model's basic application to straightforward well paths.
- Segmented trajectory wells, including designs where the wellbore is discretized into two, three, four, and five segments. Within each category, two scenarios are modeled—"arc-shaped" and "zigzag."

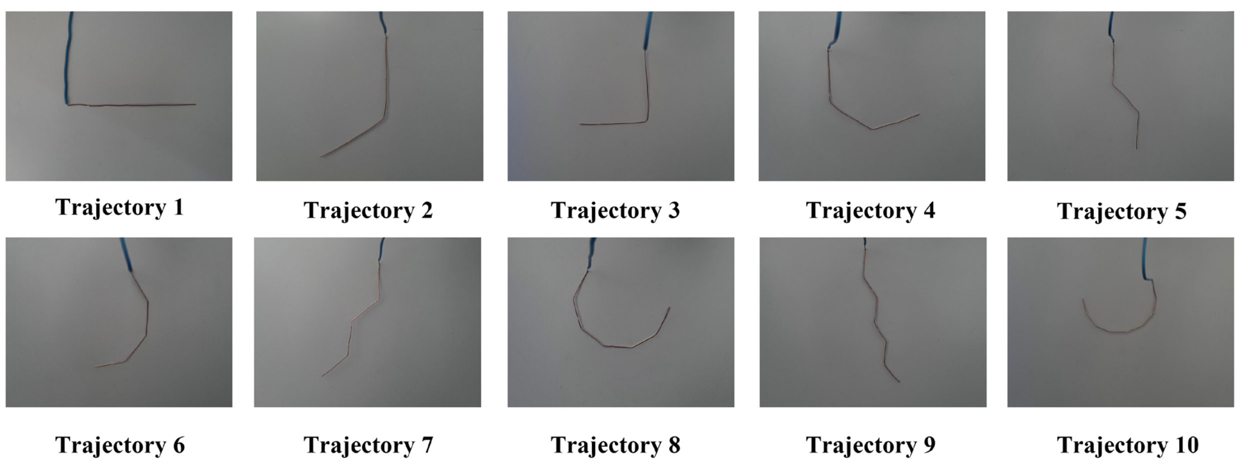

Fig. 6—Ten physical models of well trajectories in hydroelectricity simulation experiments.

These designs were selected to illustrate that the USAMF-HR model can precisely simulate both simple and complex well trajectories. By implementing a variety of well configurations, we could comprehensively test and validate the model's performance across a broad spectrum of real-world drilling conditions. The results from these simulations are detailed in **Table 1**, affirming the model's robustness and accuracy in replicating different well designs through hydraulic-electric simulation experiments.

Well Trajectory Number	Current Ratio	Productivity Ratio	Error (%)
1	1.0000	1.0000	–
2	0.9632	0.9660	0.2878
3	0.9186	0.9281	1.0279
4	0.9332	0.9382	0.5372
5	0.9229	0.9292	0.6727
6	0.7653	0.7745	1.1917
7	0.7677	0.7710	0.4280
8	0.7687	0.7691	0.0546
9	0.7663	0.7684	0.2733
10	0.7660	0.7746	1.1077

Table 1—Results of hydroelectricity simulation experiments.

Although our semi-analytical model can simulate the heterogeneity of reservoirs, the conductive medium used in hydraulic-electric simulation experiments has limitations that prevent it from fully modeling reservoir heterogeneity. Therefore, we further used numerical simulation methods (Ma et al. 2023; Krogstad et al. 2015; Almajid et al. 2021) (MRST). Initially, in a homogeneous reservoir with a horizontal permeability of 29.3 md, we randomly generated an enhancement noise between 1 md and 30 md for each grid to introduce

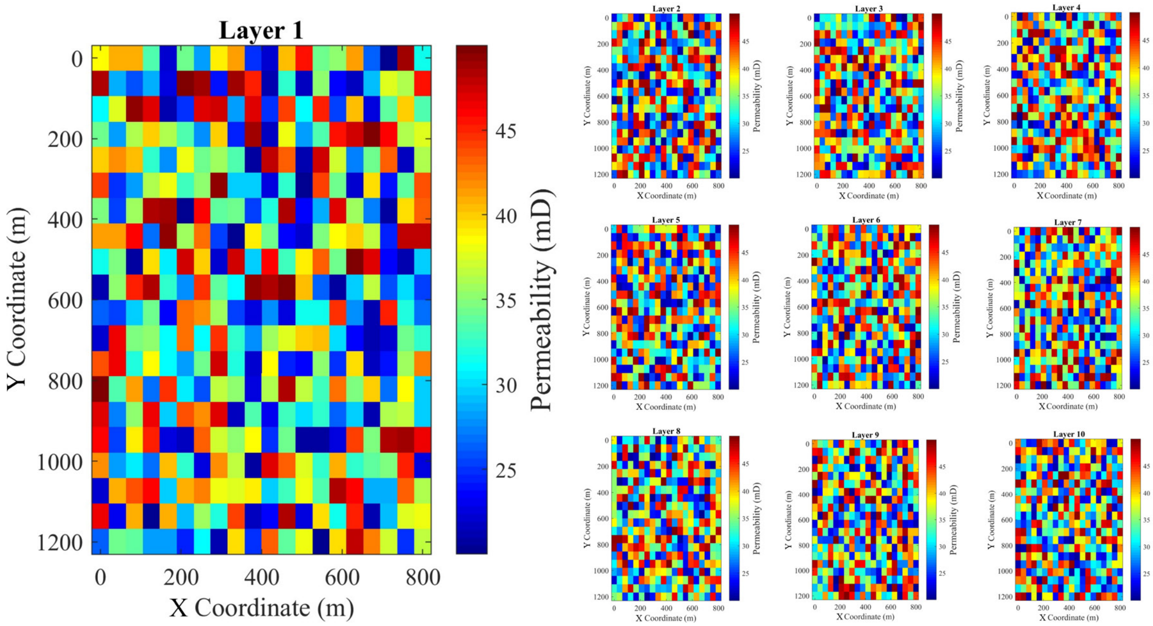

Fig. 7—Permeability distribution in 10 layers.

substantial heterogeneity into the reservoir **(Fig. 7)**. We then set up 20 simple horizontal well positions **(Fig. 8)** and calculated the oil production. Following this, we implemented the same 20 horizontal wells in our semi-analytical model and performed production calculations. The results of the comparison are shown in **Table 2**.

Position	Production Rate in MRST	Production Rate in Semi-Analytical Model	Error (%)
1	7.2	7.02	2.50
2	16.7	15.91	4.73
3	16.7	17.35	3.89
4	12.9	12.30	4.65
5	11.7	12.21	4.36
6	5.1	4.93	3.33
7	13.8	14.54	5.36
8	8.8	8.38	4.77
9	9.4	9.02	4.04
10	10.4	10.27	1.25
11	15.7	16.41	4.52
12	23.6	22.76	3.56
13	21.8	21.12	3.12
14	24.5	25.03	2.16
15	25.4	26.60	4.72
16	18.4	17.56	4.57
17	23.4	22.78	2.65
18	23.0	22.35	2.83
19	27.8	28.98	4.24
20	29.7	30.57	2.93

Table 2—Results of MRST and semianalytical model.

We validated the performance of USAMF-HR in describing unconventional wells and reservoir heterogeneity through hydroelectric simulation experiments and reservoir numerical simulation. To further assess the framework's production prediction effectiveness and practical application value for naturally fractured reservoirs, we chose the actual Reservoir A as a benchmark for model validation. Considering our focus on single-well analysis, a full reservoir simulation is unnecessary. Therefore, in our simulations, we only select one

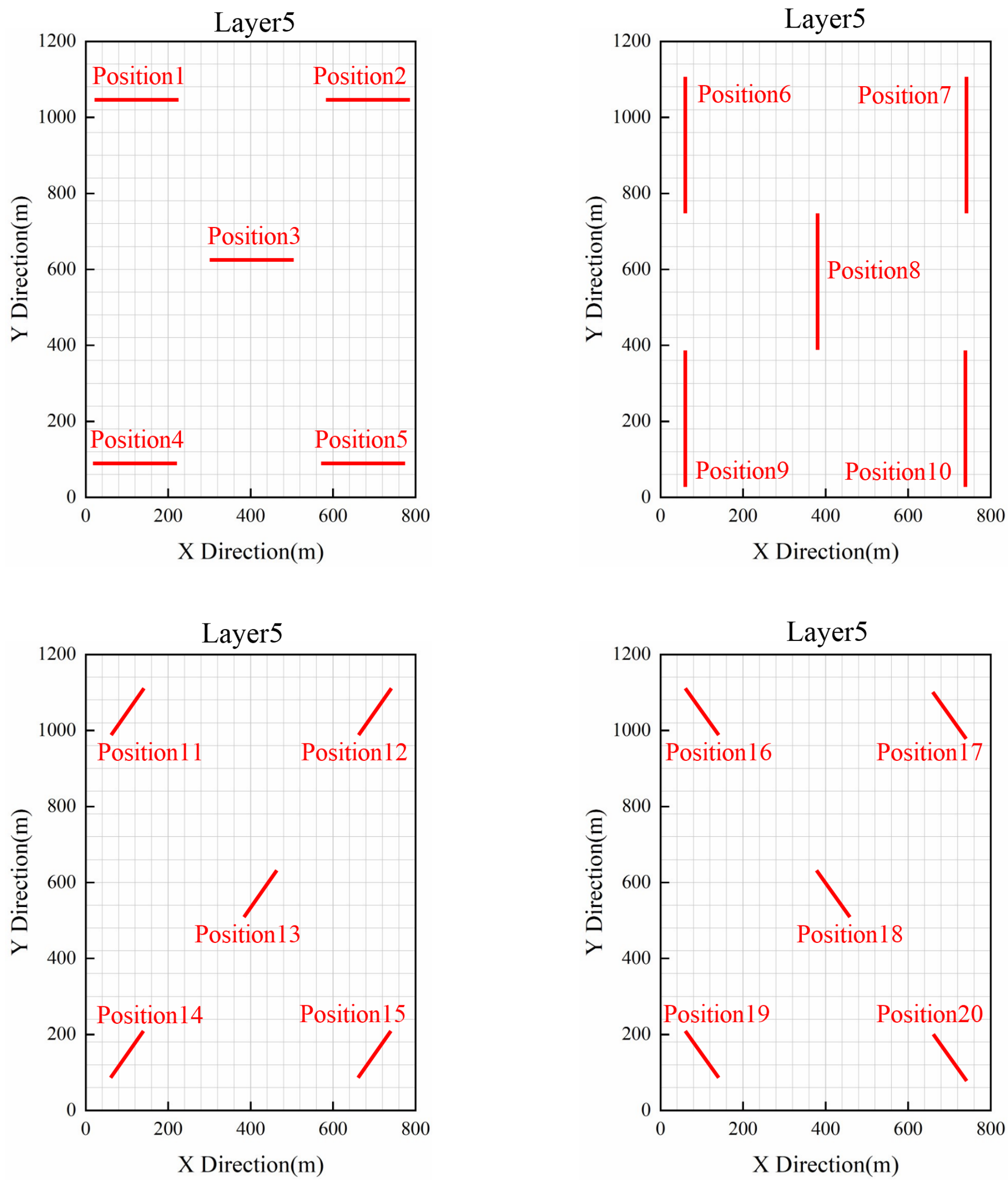

Fig. 8—Twenty horizontal well positions.

well and carve out a rectangular area around it from the entire reservoir to serve as the subject of our reservoir simulation. Using this method, we have created four different rectangular reservoir cases for validation **(Fig. 9)**.

We predicted oilwell production for the four cases and plotted the decline curves **(Fig. 10)**. The results show that the decline curves generated by the USAMF-HR model closely match those from the numerical reservoir simulation, with an average prediction error of 5%.

Altogether, the skin factor can describe the overall characteristics near the wellbore in the reservoir, and machine learning methods are an effective means to model nonlinear relationships between variables using data. Thus, we observe that in simulations of unconventional wells and reservoirs with strong heterogeneity, USAMF-HR aligns well with the results from hydroelectric simulation experiments and numerical synthetic models, demonstrating a high accuracy with an average error within 5%. In terms of stability assessment, USAMF-HR has exhibited exceptional performance across various test scenarios, including hydroelectric simulation experiments, tests on highly heterogeneous synthetic models, and validations within actual reservoir single-well systems. Particularly in simulations of actual reservoirs, we have predicted changes in well productivity for various rectangular reservoir sections cut from the actual reservoir and conducted detailed comparisons with existing numerical simulation results. These comparisons reveal that the production decline curves calculated using USAMF-HR closely match those from numerical simulations without significant deviations. These results not only confirm the robust adaptability of USAMF-HR across different application scenarios but also verify its accuracy and stability under complex reservoir conditions.

The NPV Calculation of Production Wells. To achieve the optimal trajectory of the well, it is essential to establish a rational objective function that provides a quantitative criterion for optimization. In this paper, we aim to maximize the NPV of well production as the objective function for well trajectory optimization.

The formula for calculating NPV is expressed as follows:

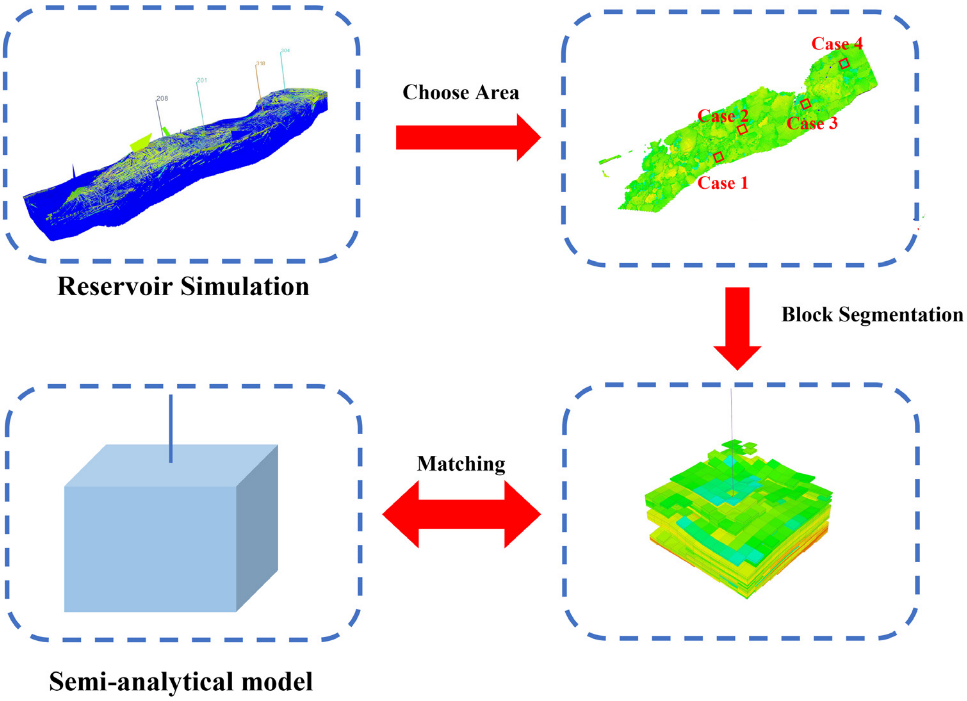

Fig. 9—Four rectangular areas extracted from actual Reservoir A to serve as comparative validation cases for the USAMF-HR framework.

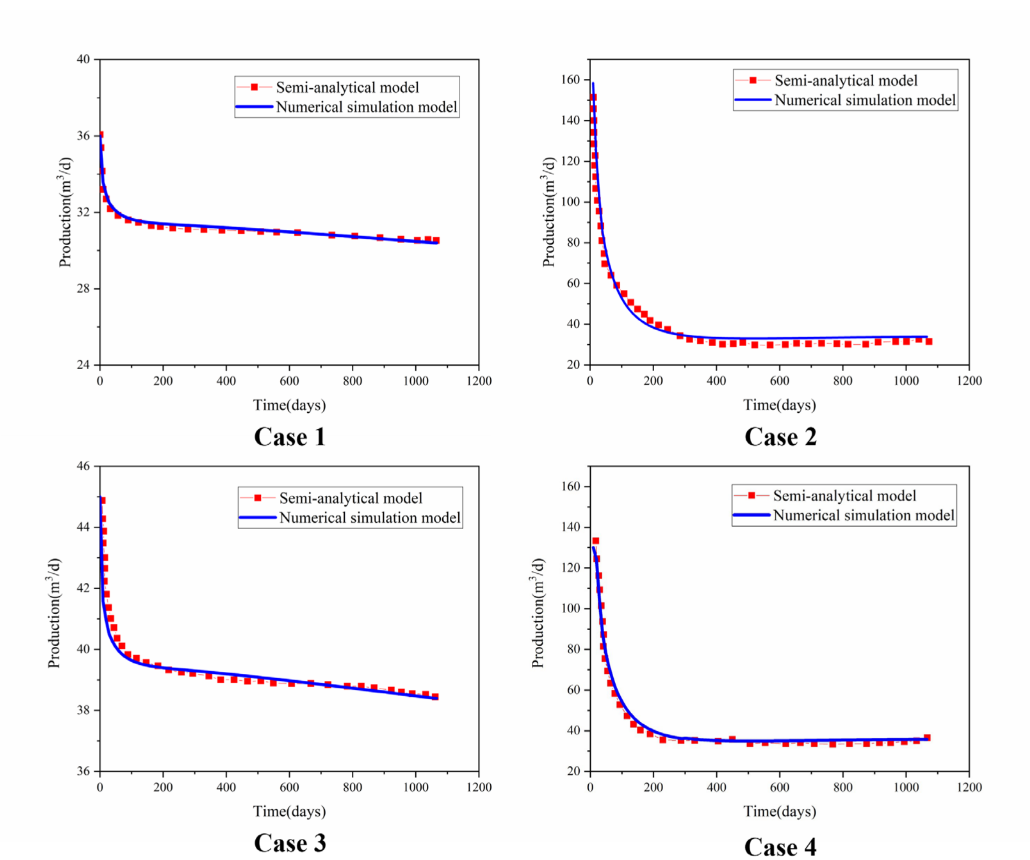

Fig. 10—Comparative results of production predictions for each case study.

$$\text{NPV} = \int_0^T \frac{Q(t)\{P(t) - P_N[Q(t)]\}}{(1+d)^t} dt - L_w P_w, \tag{12}$$

where $Q(t)$ is the production at time t, $P(t)$ is the oil price at time t, P_N is the total price of material and energy consumed per unit production of the well, L_w is the length of the completion section, P_w is the price per unit length of the wellbore, T is the total production time, and d is the discount rate, which is usually a value determined based on market interest rate, project risk, company capital cost, and other factors.

Given that the decline in oilwell production is constrained by the actual reservoir flow characteristics, it typically exhibits an exponential decay pattern. When fluctuations in oil prices and discount rates are minimal, the NPV function tends to exhibit characteristics of rapid decline followed by stabilization. In this context, we opt for the Gauss-Laguerre quadrature formula to compute cumulative production, effectively capturing this trend.

$$\text{NPV} \approx \sum_{k=1}^{n} A_k \frac{Q_k\{P_k - P_{Nk}\}}{(1+d)^k} - L_w P_w. \tag{13}$$

In the formula, A_k represents the Laguerre-Gauss quadrature coefficients, which can be obtained from standard tables during numerical integration.

Therefore, the objective function can be expressed as

$$\min \text{NPV} = \sum_{k=1}^{n} A_k \frac{Q_k\{P_k - P_{Nk}\}}{(1+d)^k} - L_w P_w. \tag{14}$$

Wellbore Trajectory Optimization Based on PSO Algorithm. In this section, we apply the PSO algorithm to well trajectory optimization, integrating it with a semi-analytical production prediction model and an NPV calculation method to form a new model for optimizing well trajectories. PSO (Liu et al. 2018) is a search algorithm based on group collaboration, proposed by Eberhart and Kennedy in 1995, inspired by the foraging behavior of birds (Kennedy and Eberhart 1995). In PSO, each search agent is treated as a "particle" with no mass and volume, flying through the solution space in search of the optimal solution. Particles update their velocity and position based on individual experience and information shared within the group (Al-Janabi et al. 2021; Feng et al. 2019). Due to its simplicity of implementation, high computational efficiency, few parameters, and ease of adjustment, PSO is particularly suited for continuous space optimization problems, effectively enhancing the scientific accuracy and precision of the optimization process (Khan et al. 2018; Sanghyun and Stephen 2018; Yao et al. 2021; Wang et al. 2023).

Rationalize the Initial Wellbore Trajectory. The model first establishes a reservoir box in the reservoir for analysis and sets multiple initial well trajectories within this box as the initial particles for the PSO algorithm. To ensure the correct operation of the model, it is extremely important to ensure that the initial well trajectory is reasonable. The model adopts the following three methods to ensure the rationality of the initial well trajectory **(Fig. 11)**.

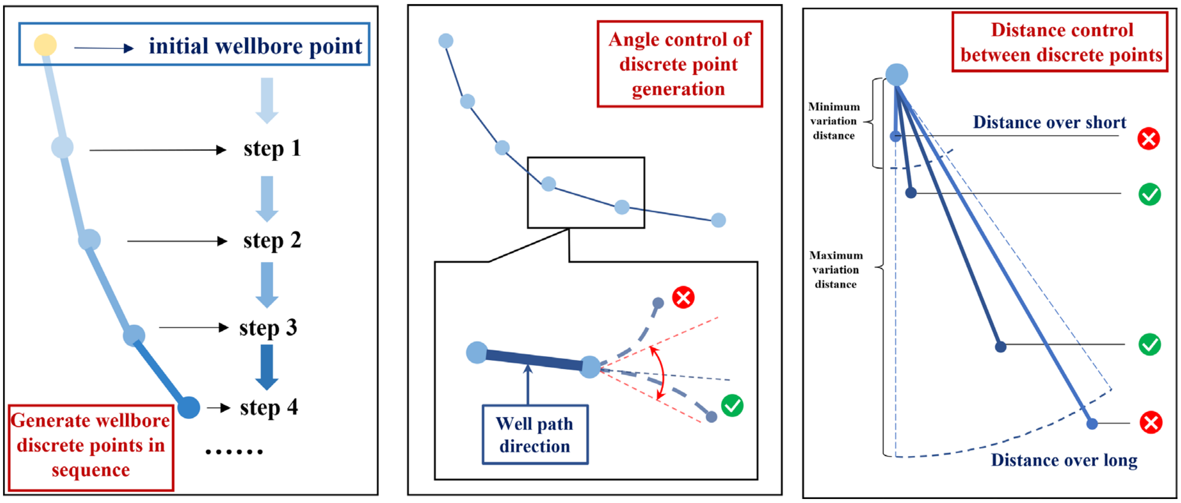

Fig. 11—Rationalize the initial well trajectory.

1. *Generate wellbore discrete points in sequence*: In the semi-analytical production prediction model, to control the shape of the wellbore, it is discretized into multiple segments, which are connected by a series of discrete points generated in sequence. This method of sequential generation not only ensures the smoothness of the trajectory but also guarantees the accuracy of the extension direction. Specifically, the initial wellbore point is first generated, and then the position of the next point is calculated based on predetermined angle and distance parameters. This process is repeated until a complete well trajectory is formed. Such a method of sequential generation helps to prevent the random distribution of discrete points, thus avoiding disordered trajectories and ensuring that each point's position precisely corresponds to its optimal path within the reservoir.
2. *Angle control of discrete point generation*: To ensure the continuity of the well trajectory and the feasibility of construction, the change in angle between adjacent wellbore discrete points must be strictly controlled. During the sequential generation of wellbore discrete points, each new point is based on the previous one and determined by setting a specific step length and angle. It is crucial

that the angle set for the new point changes only slightly compared to the angle of the previous point. This control strategy prevents sharp bends in the well trajectory, which is essential for the smooth progress of construction. Excessive changes in angle can not only increase construction difficulty but also cause damage to drilling equipment or reduce drilling efficiency. By implementing this method, the generated well trajectory will be smoother, ensuring the continuity and safety of the construction process.

3. *Distance control between discrete points*: After specifying that the angle of the discrete points can be changed, the distance between the discrete points is limited to a certain range to prevent the problem of low model accuracy caused by the large distance between the two adjacent discrete points. In this study, the distance between discrete points is set to the same value to simplify the operation process of the model and improve the operation speed.

Limit the Moving Speed and Displacement of Particles. After determining the initial well trajectory, we use a semi-analytical model and NPV calculation method to evaluate the optimal NPV values of all particles. Subsequently, through iterative calculations, other particles are gradually guided toward the position of the particle with the optimal NPV, and the NPV value and spatial position of this optimal particle are continuously updated during the iteration process. The entire iterative process follows the basic update strategy of the PSO algorithm, specifically reflected in Eqs. 15 and 16. To ensure the rationality and efficiency of the iterative updates, we have appropriately restricted the movement speed and displacement of the particles.

$$\vec{v}_i^{(t+1)} = \omega \vec{v}_i^{(t)} + c_1 T_1 \left(\vec{p}_{\mathrm{best},i} - \vec{x}_i^{(t)} \right) + c_2 T_2 \left(\vec{g}_{\mathrm{best},i} - \vec{x}_i^{(t)} \right), \tag{15}$$

$$\vec{x}_i^{(t+1)} = \vec{x}_i^{(t)} + \vec{v}_i^{(t+1)}, \tag{16}$$

where $\vec{p}_{\mathrm{best},i}$ is the best position iterated by particle i so far, and $\vec{g}_{\mathrm{best},i}$ is the best position found by all particles in the whole population. The parameter ω is the inertial weight, which controls the particle search range. c_1 and c_2 are acceleration constants, which determine the influence of individual and group experience on the velocity. T_1 and T_2 are random numbers to keep the search random and diverse.

1. *Update strategy for nonglobally optimal particles*: For nonglobally optimal particles, it is necessary to gradually approach the globally optimal particle during each iteration update. To prevent undesirable deformations in the well trajectory during the update process, we take the following measures: First, the algorithm calculates the geometric center point of the well trajectory and establishes a movement vector pointing toward the globally optimal position based on this. Subsequently, the entire well trajectory is translated along this vector, ensuring that the overall shape of the well trajectory remains stable throughout the iteration process. This method not only ensures the directionality of the updates but also prevents potential structural collapses of the well trajectory.
2. *Speed adjustment based on boundary constraints*: In the PSO algorithm, the velocity of a particle is defined as the change in its displacement from the original position after each iteration update. Because all particles must always remain within the designated reservoir box, we have set an upper limit on the velocity of the particles to prevent excessive jumping during the search process, which could affect the stability and efficiency of the algorithm. This constraint not only ensures the continuity and effectiveness of the search but also prevents particles from exceeding the predetermined search boundaries.
3. *Fine-tuning of globally optimal particles*: To enhance the accuracy of the algorithm, we finely adjust the position of the globally optimal particle during the movement of nonglobally optimal particles. We keep the position of the first discrete point unchanged and use it as the center point to make slight rotational adjustments to the well trajectory represented by the globally optimal particle. This method allows us to explore whether there are better solutions around the globally optimal particle. The adjustment process and its results are displayed in **Fig. 12**.

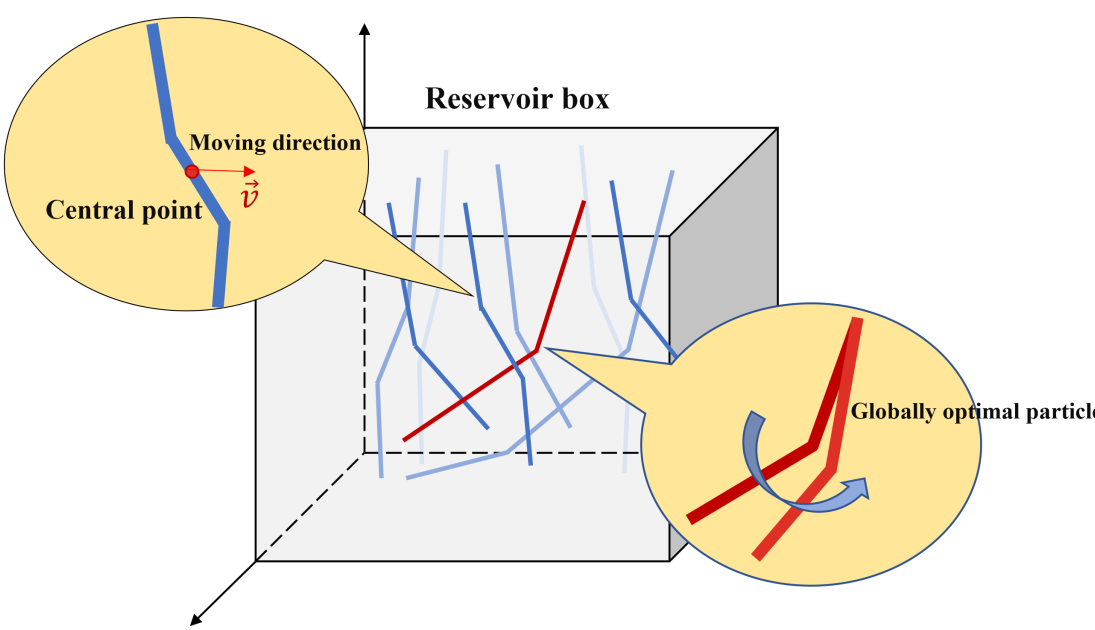

Fig. 12—Update strategies for globally optimal and nonglobally optimal particles.

To fully comply with the three constraints during the optimization process, we meticulously designed specific restriction functions and conditional statements while implementing the PSO algorithm. The algorithm includes two main classes—the particle class and the particle swarm optimizer class. In the particle class, conditional statements ensure that each generated particle (well trajectory) adheres to boundary constraints and that update strategies comply with these constraints. In the particle swarm optimizer class, a fine-tuning feature for the globally optimal particle is set up to implement and maintain the third constraint.

Parameter Setting. PSO mainly determines the initial particles and the changes of each particle in the iterative updating process by particle number, iteration times, inertia weight, acceleration constants, and other parameters (Yao et al. 2021; Wang et al. 2024). **Table 3** describes the parameters to be set.

Parameters	Value	Note
Particle number	10–1000	The value can be adjusted based on the complexity of the problem and computing resources
Iteration times	100–1000	The value can be adjusted based on the complexity of the problem and computing resources
Inertia weight	0.1–0.9	The degree to control the particle maintaining its previous direction of motion during the search process, usually taking the value around 0.5
Acceleration constants	1–2	Used to adjust the movement speed of particles in the search space

Table 3—Particle swarm algorithm parameter setting range.

It should be noted that the setting of parameters in the PSO algorithm will affect the performance of the algorithm, so it needs to be adjusted according to specific problems to obtain better optimization results.

Simulated Case Study

To comprehensively demonstrate the implementation process of the method described in this paper and to verify its effectiveness in optimizing well trajectories in naturally fractured reservoirs, we have selected the four individual blocks of Reservoir A mentioned in the model validation section as simulation cases.

Reservoir Model and Parameter Description. First, we need to establish semi-analytical models for the four cases mentioned above. Because all these actual cases involve heterogeneous naturally fractured reservoirs and semi-analytical models struggle to fully capture the complex characteristics of heterogeneous reservoirs, we initially describe the reservoirs in each case as homogeneous yet anisotropic boxes. The detailed parameters and assumptions involved in this process are listed in **Table 4**.

Parameters	Case 1	Case 2	Case 3	Case 4
Reservoir length (m)	963	963	962	911
Reservoir width (m)	963	962	1043	833
Reservoir height (m)	564.95	734.56	671.98	546.73
Top depth of reservoir (m)	2798.27	2642.14	2713.38	2821.5
Oil density (kg/m^3)	830	830	830	830
Volume coefficient	1.11	1.11	1.11	1.11
Oil viscosity (mPa·s)	1.083	1.083	1.083	1.083
Compressibility of fluid (MPa^{-1})	2.39×10^{-3}	2.39×10^{-3}	2.39×10^{-3}	2.39×10^{-3}
Compressibility of rock (MPa^{-1})	3.00×10^{-5}	3.00×10^{-5}	3.00×10^{-5}	3.00×10^{-5}
Porosity (%)	6.06	6.06	6.06	3.78
Boundary pressure (MPa)	36	36	36	36
Permeability in the *x*-direction (md)	0.35	0.21	0.16	0.26
Permeability in the *y*-direction (md)	0.35	0.21	0.16	0.26
Permeability in the *z*-direction (md)	2.00×10^{-4}	2.00×10^{-4}	2.00×10^{-4}	2.00×10^{-4}

Table 4—Basic parameters for the four cases.

To describe the reservoir's heterogeneity, in the USAMF-HR framework, we generated a data set of discrete unit positions and skin factors by combining reservoir numerical simulation and optimization algorithms. By using neural networks to predict the skin factors of discrete units, we effectively overcome the limitations of semi-analytical models in simulating reservoir heterogeneity.

After thoroughly describing the physical and geological characteristics of the reservoir, we also considered economic factors. Based on the current international crude oil price, we set the oil price at USD 82.32/bbl, drilling cost at USD 420.53/m, a discount rate of 0.08 to 0.2, and the total material and energy cost for unit production consumption of the oil well at USD 280.35/m.

Well Trajectory Optimization Settings. During the optimization process, the determination of the inertia weight and acceleration constants is crucial for the convergence speed and accuracy of the PSO results. Therefore, we selected Case 1 as our study object and investigated several common methods for setting inertia weights and acceleration constants. Through sensitivity analysis, we identified the most appropriate parameter settings and applied them to other case studies to ensure the consistency and reliability of the optimization results.

Fig. 13 (left) presents a sensitivity analysis of various methods for selecting the inertia weight ω. The inertia weight ω indicates the particle's tendency to retain its previous velocity, with a larger inertia weight favoring global searches and a smaller one favoring local searches. We evaluated two fixed weights ($\omega = 0.1$ and $\omega = 0.9$), a linearly changing weight (Eq. 17), and two nonlinearly changing weights (Eqs. 18 and 19). The results indicate that dynamically adjusted weights significantly outperform fixed weights, with the second nonlinear weight showing the best performance.

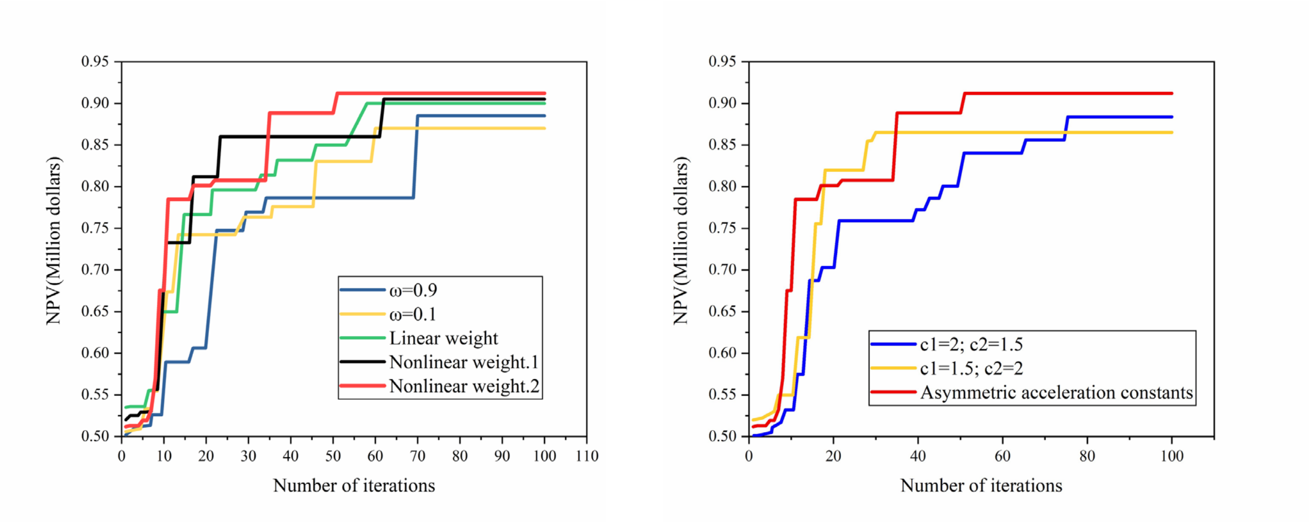

Fig. 13—Sensitivity analysis of PSO parameters for Case 1, showing inertia weights (left) and acceleration constants (right).

$$\omega(k) = \omega_{\text{start}} - (\omega_{\text{start}} - \omega_{\text{end}}) \times \frac{k}{T_{\max}}, \tag{17}$$

$$\omega(k) = \omega_{\text{start}} - (\omega_{\text{start}} - \omega_{\text{end}}) \times \left(\frac{k}{T_{\max}}\right)^2, \tag{18}$$

$$\omega(k) = \omega_{\text{start}} - (\omega_{\text{start}} - \omega_{\text{end}}) \times \left[\frac{2k}{T_{\max}} - \left(\frac{k}{T_{\max}}\right)^2\right]. \tag{19}$$

In the formula, ω_{start} represents the initial inertia weight, set to 0.9; ω_{end} is the inertia weight when iteration reaches its maximum, set to 0.1; the variable k denotes the current iteration number; and $T_{\max}$ is the maximum number of iterations, set to 100.

Fig. 13 (right) performs a sensitivity analysis on the selection methods for acceleration constants c_1 and c_2, which collectively determine how particles adjust their trajectories based on personal and collective experience. A higher c_1 value leads to excessive local search by particles, while a higher c_2 value encourages premature convergence to local optima. Introducing the asymmetric acceleration constants method (Eqs. 19 and 20) addresses the optimal selection of c_1 and c_2 throughout the optimization process. This method displayed the best optimization outcomes in the graph.

$$c_1^k = c_1^{\text{ini}} + (c_1^{\text{fin}} - c_1^{\text{ini}}) \times \frac{k}{T_{\max}}, \tag{20}$$

$$c_2^k = c_2^{\text{ini}} + (c_2^{\text{fin}} - c_2^{\text{ini}}) \times \frac{k}{T_{\max}}. \tag{21}$$

In the formula, c_1^{ini} is the initial value for the individual speed factor, set at 2; c_1^{fin} is the final value for the individual speed factor, set at 1; c_2^{init} is the initial value for the social speed factor, set at 1; and c_2^{fin} is the final value for the social speed factor, set at 2.

In summary, given that all cases originate from similar stratum data with comparable reservoir properties, we have chosen the second nonlinear inertia weight method and the asymmetric acceleration constants method as our strategy for parameter settings, ensuring consistency and optimal performance across various cases.

Next, we generated a set of initial particles, each representing a different initial well trajectory. Given the large number of particles, we have selected only 10 initial well trajectories for display **(Fig. 14)**. In the actual optimization process, field engineers can propose several well trajectory options that are likely to be effective based on their experience and the characteristics of the reservoir. This approach not only ensures the effectiveness of the optimization but also helps to accelerate the convergence speed of the process.

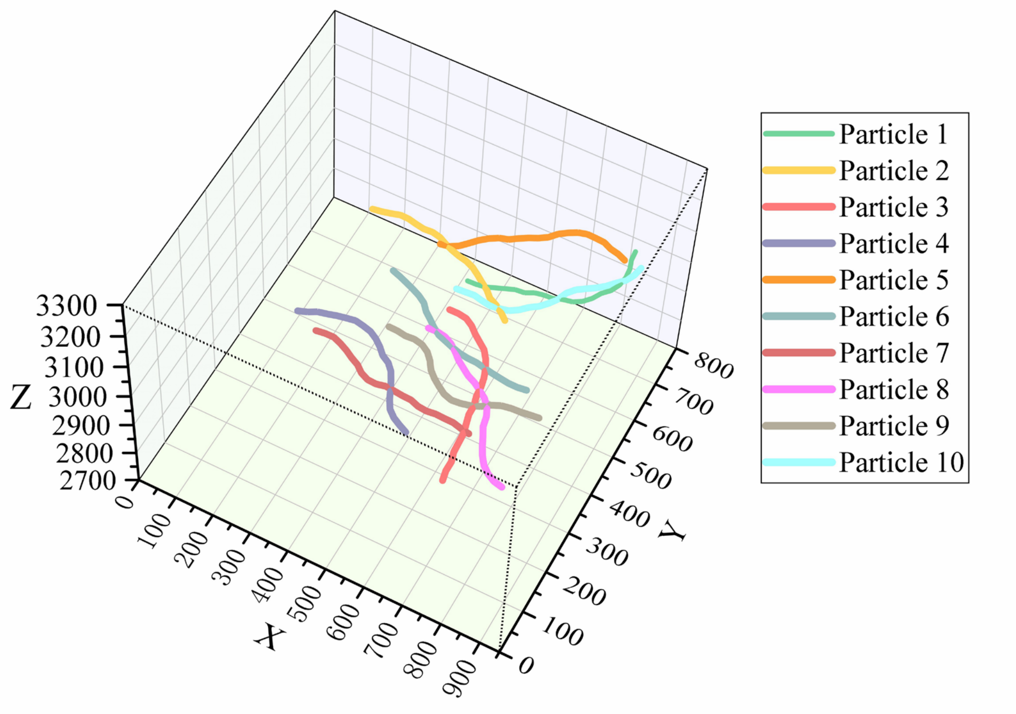

Fig. 14—Initial well trajectory (part).

Optimization Outcomes. In this section, we conduct a detailed analysis and summary of the optimization results, explore the feasibility of the well trajectory optimization method for naturally fractured reservoirs proposed in this paper, and evaluate its optimization effects.

Fig. 15 displays the variation curves of local and global optimal NPVs throughout the iterations in four repeated experiments of PSO conducted on Case 1. Despite variations due to the stochastic nature of the optimization algorithm, the differences among the final global optimal NPVs are minor. Taking the first experiment as an example, it can be observed that the locally optimal NPV curve is highly volatile, reflecting the exploration of various well trajectory configurations throughout the optimization process, with fluctuations likely due to frequent solution adjustments based on local information. In contrast, the globally optimal NPV curve shows a stable, stepwise increasing trend, indicating that the algorithm consistently found superior solutions as iterations progressed, achieving the global optimum in the 51st iteration. This comparison reveals the algorithm's capability to gradually improve solution quality while maintaining a balance between exploration and exploitation in practical optimization tasks.

It is important to note that **Fig. 15** shows slight variations in the global optimal solutions across experiments. This is primarily because the current simulation experiment was conducted for only 100 iterations, so the global optimum obtained may not be the actual optimum. Additionally, the initial well trajectories in the experiment were randomly generated within a certain range, which lacks sufficient scientific basis and thus may prevent the optimization process from converging quickly and stably. The main objective of this study is to demonstrate the auto-optimization capability of the proposed well trajectory optimization method rather than to solve for an exact global optimum under current conditions. By integrating field expert experience to optimize the initial well trajectory settings and increasing the number of iterations, we believe this method will demonstrate greater practical application value.

Fig. 16 shows the optimal well trajectories corresponding to the locally optimal solutions at each iteration during the first experiment of Case 1. Due to the large number of iterations, for clarity, we have selected a set of data every 10 iterations to plot the well trajectory curves. In this case, the global optimal NPV occurred in the 51st iteration and is marked in red. It is evident from the figure that the optimal well trajectory is continuously optimized with each iteration, with the algorithm actively exploring around the optimal well trajectory, gradually approaching the direction of the best well trajectory.

For the first experiment of Case 1, we selected one particle from the initial particle swarm, a local optimal particle during the iteration process, and the global optimal particle after 100 iterations for simulation using the USAMF-HR framework. The results of these simulations are shown in **Fig. 17**.

The left panel displays the production changes over 3 years for three different well trajectories. The global best production curve, obtained after 100 iterations, shows the highest production and remains relatively stable throughout the simulation period. This indicates that the process of optimizing well trajectories successfully maximized production. Meanwhile, the production curve of the local best particle during the iterations generally exceeds that of the initial particle, further confirming the effectiveness of the PSO in finding optimal solutions.

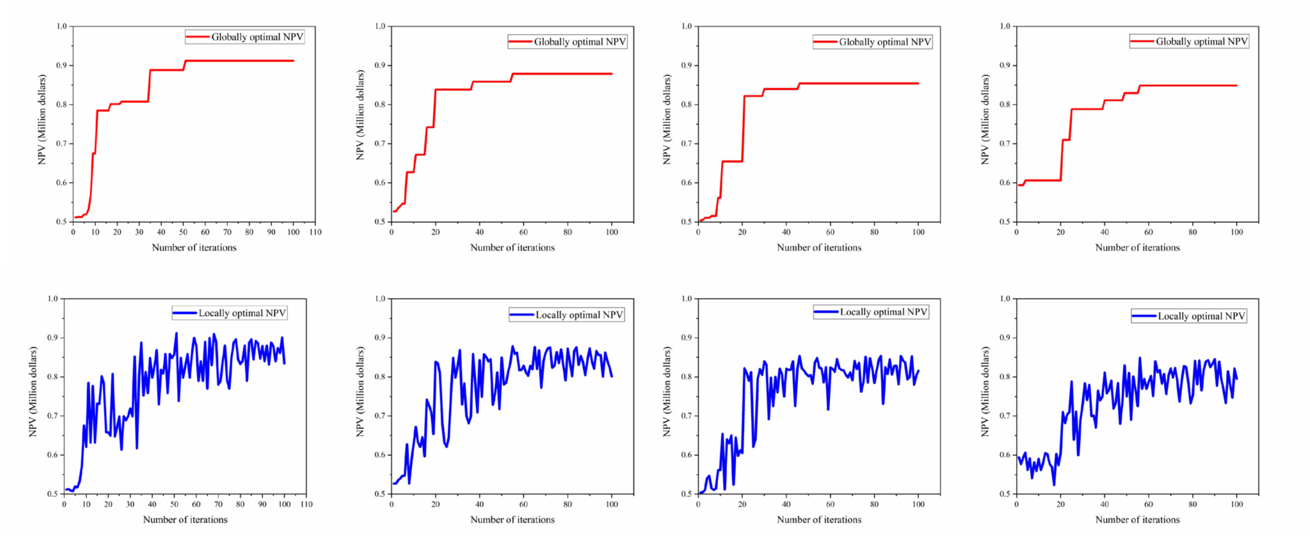

Fig. 15—Variation of local and global optimal NPV in 4 PSO trials for Case 1.

In addition to production, the cumulative production and NPV of all trajectories also show linear growth (middle and right panels). Although the simulation case presented in this paper is somewhat idealized, it does not affect the conclusions drawn. Notably, the optimized well trajectories demonstrate faster growth in cumulative production over time, thereby achieving greater economic benefits more quickly.

To validate the universality of the well trajectory optimization method proposed in this article using the PSO algorithm and the USAMF-HR framework, we conducted the same case analyses for Cases 2, 3, and 4. **Figs. 18 and 19,** respectively, show the variations of local and global optimal NPV with the number of iterations, and the changes in NPV over production time for different particles in Cases 2 to 4. The results indicate, similar to Case 1, that all three cases converged within a limited number of iterations. Moreover, compared to scenarios without PSO optimization or with insufficient iterations, the well trajectories that reached convergence demonstrated significantly superior NPV throughout the production phase.

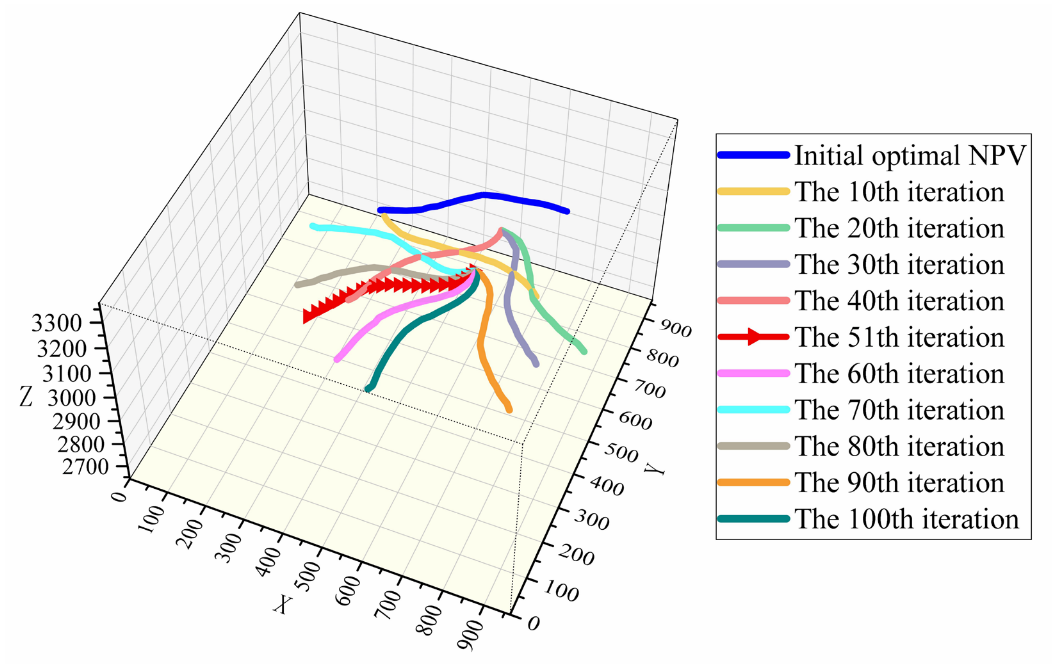

Fig. 16—Evolution of well trajectories in Case 1 during selected iterations of the first PSO experiment (part).

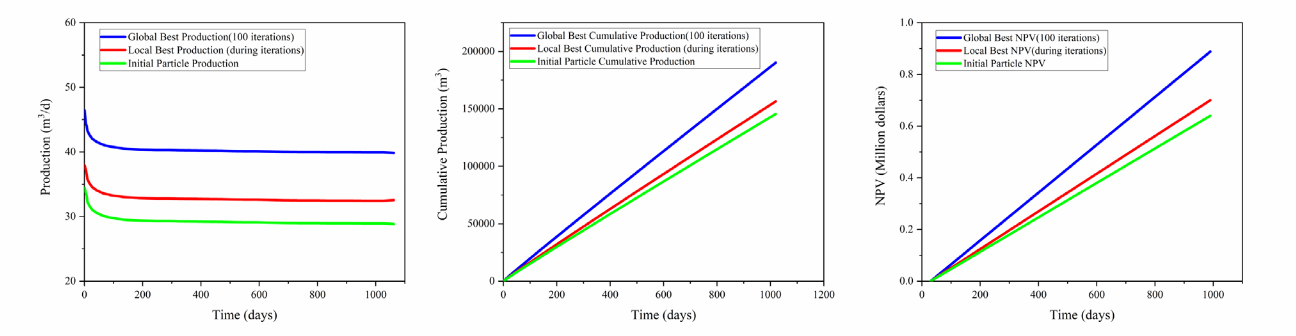

Fig. 17—Comparison of production, NPV, and cumulative production of three particles.

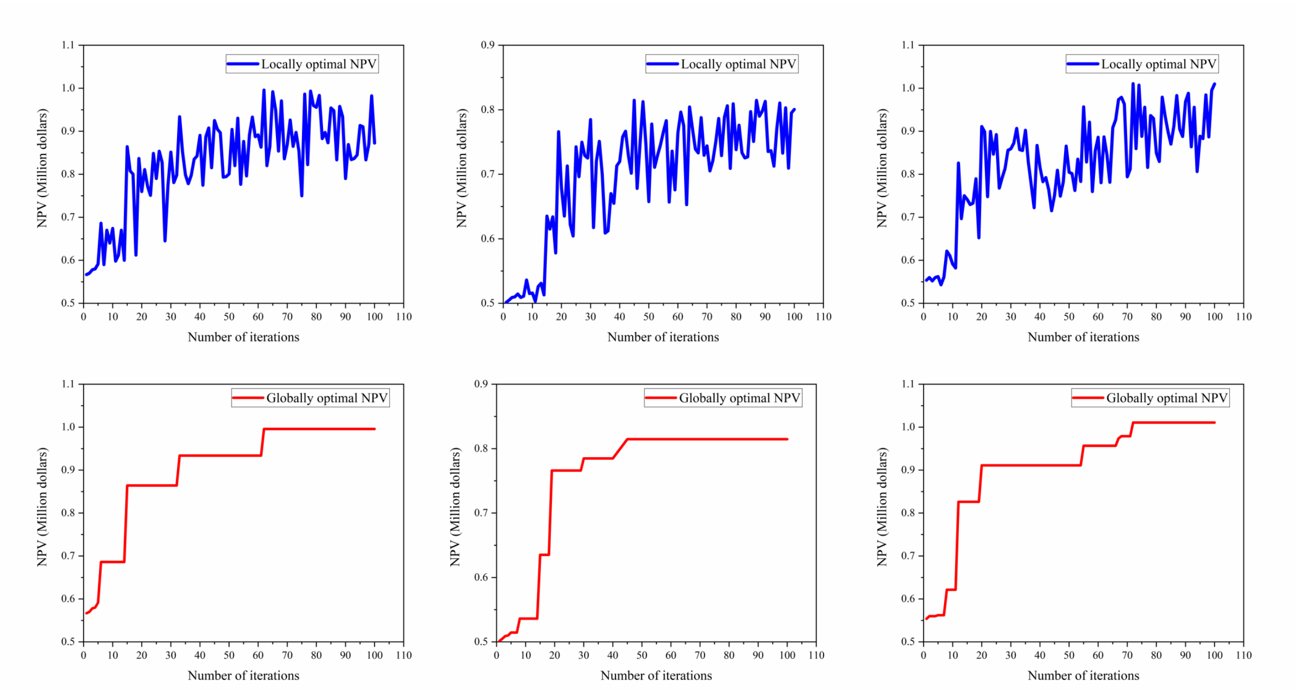

Fig. 18—Variation of local and global optimal NPV for Cases 2, 3, and 4.

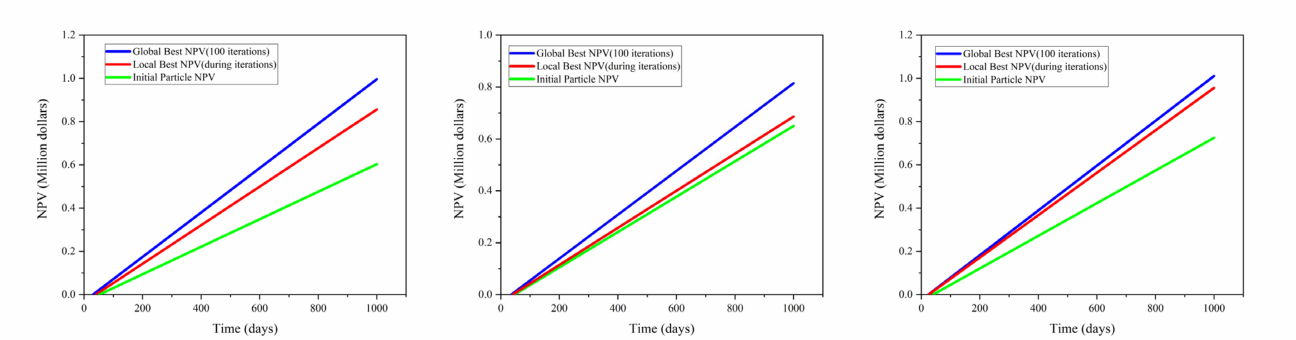

Fig. 19—Comparison of NPV of three particles for Cases 2, 3, and 4.

This case study further validates the feasibility of using the USAMF-HR framework to simulate unconventional wells in naturally fractured reservoirs, as well as the effectiveness of PSO in optimizing well trajectories. However, considering the variety of optimization algorithms available, PSO might not be the best choice. Therefore, we have also included GAs and differential evolution for performance comparison **(Fig. 20)**.

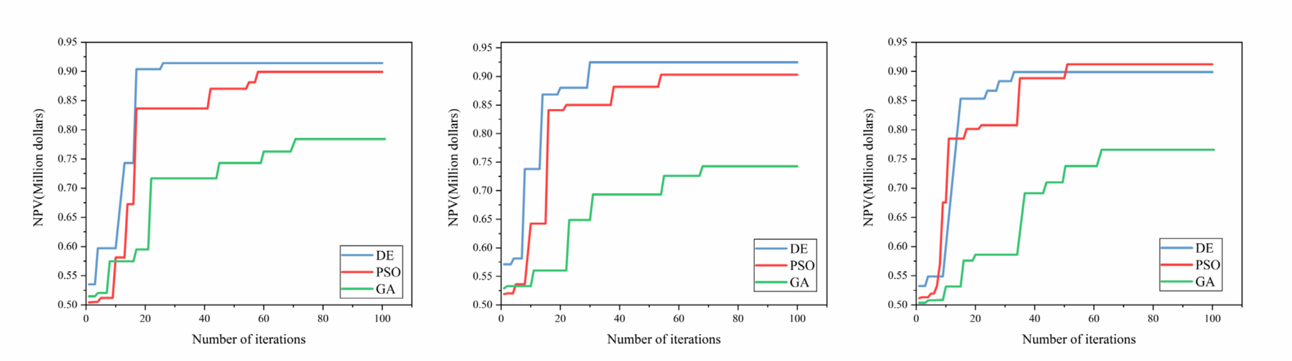

Fig. 20—Comparison of PSO, GA, and differential evolution.

GA and PSO are currently the most widely used optimization algorithms due to their simple principles and ease of implementation, which is one of the main reasons for choosing PSO as the subject of study. As observed in **Fig. 20**, PSO outperforms GA in terms of convergence speed and optimization effectiveness, mainly due to PSO's use of real-number encoding to describe well trajectories, which is more suited for finding optimal solutions in continuous spaces than GA's binary encoding. Additionally, as a newer optimization method, differential evolution demonstrates faster convergence and greater stability, suggesting that emerging optimization technologies may offer advantages over traditional methods. Based on these findings, future work will involve a broader investigation of emerging optimization algorithms, combined with the USAMF-HR framework, to select the optimal method for well trajectory optimization research.

Conclusions

1. Traditional well trajectory optimization mainly focuses on geology and drilling engineering, but in heterogeneous reservoirs such as naturally fractured ones, the design of the completion section of the well trajectory has a decisive impact on reservoir development. This study has successfully developed and validated a well trajectory optimization method suitable for naturally fractured reservoirs, using a PSO algorithm and integrating reservoir simulation, optimization techniques, and machine learning, aimed at maximizing the NPV.
2. Based on semi-analytical models and neural network technology, we have developed a new framework (USAMF-HR) that accurately describes the complex characteristics of reservoirs. Compared to full numerical simulation, this framework uses a semi-analytical approach as a reservoir simulation tool, which not only more finely describes well trajectories but also requires fewer input parameters, making the relationship between well trajectories and production more intuitive and efficient. Before constructing the semi-analytical model, we combined optimization algorithms and neural networks to successfully predict the skin factors of any discrete wellbore units, overcoming the limitations of traditional analytical models in describing reservoir heterogeneity, thus expanding the applicability of semi-analytical models. In the application of the PSO algorithm, we effectively facilitated the algorithm's rapid convergence to the global optimum by appropriately setting the initial well trajectories and restricting the movement speed and position of the particles.
3. The method proposed in this study has great potential, such as the applicability of USAMF-HR to other types of reservoirs, including unconventional shale plays or offshore oil fields. In the future, we plan to develop more advanced models and adopt more efficient optimization algorithms (such as differential evolution algorithms or surrogate-assisted evolutionary algorithms) to handle more complex reservoir conditions, aiming to achieve more refined well trajectory designs. Especially in the context of rapid development of artificial intelligence technology, compared to traditional optimization algorithms, reinforcement learning shows superior performance in establishing long-term strategies. This will be an important direction for our future research.

Acknowledgments

The authors are grateful for the financial support from the National Natural Science Foundation of China, under Project No. 52204059. The publication costs of this article were partially covered by Jin Shu.

References

Al-Aruri, A., Iskakov, E., and Park, H. Y. 2022. Development of Gas Injection Strategy Optimized Under Subsurface Uncertainties in Naturally Fractured Karachaganak Reservoir. Paper presented at the SPE Annual Caspian Technical Conference, Nur-Sultan, Kazakhstan, 15−17 November. https://doi.org/10.2118/212061-MS.

Al-Janabi, M. A., Al-Fatlawi, O. F., Sadiq, D. J. et al. 2021. Numerical Simulation of Gas Lift Optimization Using Artificial Intelligence for a Middle Eastern Oil Field. Paper presented at the Abu Dhabi International Petroleum Exhibition & Conference, Abu Dhabi, UAE, 15−18 November. https://doi.org/10.2118/207341-MS.

Almajid, M. M., AlYousef, Z. A., and Swaie, O. S. 2021. Local Equilibrium Mechanistic Simulation of CO_2-Foam Flooding. Paper presented at the SPE Reservoir Simulation Conference, On-Demand, 26 October. https://doi.org/10.2118/203922-MS.

Apisaksirikul, S. and Blasingame, T. A. 2016. The Development and Application of a New Semi-Analytical Model to Estimate Permeability from Mercury Injection Capillary Pressure. Paper presented at the SPE/AAPG/SEG Unconventional Resources Technology Conference, San Antonio, Texas, USA, 1−3 August. https://doi.org/10.15530/urtec-2016-2460639.

Bazalgette, L., Aamri, N., Field, C. et al. 2022. Natural Fractures Help Unlocking Tight Carbonates: Re-Developing the Natih B Reservoir in a Giant Field in the Sultanate of Oman. Paper presented at the ADIPEC, Abu Dhabi, UAE, 31 October–3 November. https://doi.org/10.2118/211336-MS.

Cao, C., Cheng, L., Jia, Z. et al. 2022. An Integrated Model Combining Complex Fracture Networks and Time-Varying Data Modeling Techniques for Production Performance Analysis in Tight Reservoirs. Paper presented at the SPE EuropEC - Europe Energy Conference Featured at the 83rd EAGE Annual Conference & Exhibition, Madrid, Spain, 6−9 June. https://doi.org/10.2118/209632-MS.

Chen, D., Mao, K., Ye, Z. et al. 2024. An Artificial Intelligent Well Trajectory Design Method Combining Both Geological and Engineering Objectives. *Geoenergy Sci Eng* **236**: 212736. https://doi.org/10.1016/j.geoen.2024.212736.

Clarkson, C. R., Williams-Kovacs, J. D., Qanbari, F. et al. 2014. History-Matching and Forecasting Tight/Shale Gas Condensate Wells Using Combined Analytical, Semi-Analytical, and Empirical Methods. Paper presented at the SPE/CSUR Unconventional Resources Conference – Canada, Calgary, Alberta, Canada, 30 September–2 October. https://doi.org/10.2118/171593-MS.

Cui, Y., Zhang, F., Jiang, R. et al. 2022. Pressure Transient Behavior Modeling of a Multi-Horizontal Well Pad with Damaged Fracture in Shale Gas. *J Pet Sci Eng* **216**: 110755. https://doi.org/10.1016/j.petrol.2022.110755.

Dou, Z.-J., Liu, Y.-S., Qin, X. et al. 2022. Multi-Objective Optimization Design of Deviation-Correction Trajectory Considering the Production Loss in Shale Gas Cluster Well. *Pet Sci* **19** (6): 2995–3003. https://doi.org/10.1016/j.petsci.2022.09.024.

Feng, C., Li, J., Feng, Z. et al. 2019. Predict Oil Production from Geological and Petrophysical Data Before Hydraulic Fracturing Using an Improved Particle Swarm Optimization Based Least Squares Support Vector Machine. Paper presented at the Abu Dhabi International Petroleum Exhibition & Conference, Abu Dhabi, UAE, 11−14 November. https://doi.org/10.2118/197250-MS.

Ghadami, S., Biglarian, H., Beyrami, H. et al. 2022. Optimization of Multilateral Well Trajectories Using Pattern Search and Genetic Algorithms. *Res Eng* **16**: 100722. https://doi.org/10.1016/j.rineng.2022.100722.

Grechishnikova, A. 2016. Discrete Fracture Network Model Developed from a High Resolution LIDAR Outcrop Survey of a Naturally Fractured Unconventional Niobrara Reservoir, Denver Basin. Paper presented at the SPE/AAPG/SEG Unconventional Resources Technology Conference, San Antonio, Texas, USA, 1−3 August. https://doi.org/10.15530/urtec-2016-2430655.

Gu, Y., Gao, D., Diao, B. et al. 2022. Optimization Design Method of Infill Well Trajectory with Bypassing Obstacles in the Fractured Area of Shale Gas Reservoir. *J Pet Sci Eng* **208**: 109779. https://doi.org/10.1016/j.petrol.2021.109779.

Han, X., Xiong, C., Yang, Z. et al. 2019. Mechanism of Natural Fractures Opening in Ultra-Deep Fractured Reservoir during Stimulation. Paper presented at the 5th ISRM Young Scholars' Symposium on Rock Mechanics and International Symposium on Rock Engineering for Innovative Future, Okinawa, Japan, 1−4 December. ISRM-YSRM-2019-024.

Jiang, L., Liu, J., Liu, T. et al. 2020. Semi-Analytical Modeling of Transient Pressure Behaviour for a Fractured Vertical Well with Hydraulic/Natural Fracture Networks by Considering Stress-Sensitive Effect. *J Nat Gas Sci Eng* **82**: 103477. https://doi.org/10.1016/j.jngse.2020.103477.

Kasravi, J., Safarzadeh, M. A., and Hashemi, A. 2017. A Population-Feedback Control Based Algorithm for Well Trajectory Optimization Using Proxy Model. *J Rock Mech Geotech Eng* **9** (2): 281–290. https://doi.org/10.1016/j.jrmge.2016.07.010.

Kennedy, J. and Eberhart, R. 1995. Particle Swarm Optimization. Paper presented at the ICNN'95 - International Conference on Neural Networks, Vol. 4, 1942–1948, Perth, WA, Australia. https://doi.org/10.1109/ICNN.1995.488968.

Khan, M. R., Sadeed, A., Asad, A. et al. 2018. Maximizing Oil Recovery in a Naturally Fractured Carbonate Reservoir Using Computational Intelligence Based on Particle Swarm Optimization. Paper presented at the PAPG/SPE Pakistan Section Annual Technical Conference and Exhibition, Islamabad, Pakistan, 10−12 December. https://doi.org/10.2118/195664-MS.

Krogstad, S., Lie, K., Møyner, O. et al. 2015. MRST-AD – an Open-Source Framework for Rapid Prototyping and Evaluation of Reservoir Simulation Problems. Paper presented at the SPE Reservoir Simulation Symposium, Houston, Texas, USA, 23−25 February. https://doi.org/10.2118/173317-MS.

Li, Y., ONeal, R., Whitezell, M. et al. 2024. Optimizing Injection Well Trajectory to Maximize Storage Security and Minimize Geomechanical Risk. Paper presented at the SPE Western Regional Meeting, Palo Alto, California, USA, 16−18 April. https://doi.org/10.2118/218884-MS.

Liu, H., Gjersvik, T. B., and Faanes, A. 2022. Subsea Field Layout Optimization (Part I) – Directional Well Trajectory Planning Based on 3D Dubins Curve. *J Pet Sci Eng* **208**: 109450. https://doi.org/10.1016/j.petrol.2021.109450.

Liu, B., Mohandes, M., and Nuha, H. 2018. Seismic-Model Estimation Using Particle-Swarm Optimization. Paper presented at the SEG Technical Program Expanded Abstracts 2018, SEG Technical Program Expanded Abstracts 2018, Anaheim, California, USA.

Lyngra, S., Widjaja, D. R., Al-Shammeri, F. M. et al. 2015. A Complex Naturally Fractured Reservoir Case Study: Fracture System Understanding Is Key to Development Drilling Success. Paper presented at the SPE Saudi Arabia Section Annual Technical Symposium and Exhibition, Al-Khobar, Saudi Arabia, 21−23 April. https://doi.org/10.2118/178011-MS.

Ma, T., Zhang, D., Yang, M. et al. 2023. Fracture Pressure Prediction by Using the LSTM Neural Network Model. Paper presented at the 57th U.S. Rock Mechanics/Geomechanics Symposium, Atlanta, Georgia, USA, 25−28 June. https://doi.org/10.56952/ARMA-2023-0069.

Mienzan, F. K. and Asumadu, D. Y. 2020. Gas Rate-Decline Type Curve Analysis Using a Semi-Analytical Model. Paper presented at the SPE Nigeria Annual International Conference and Exhibition, Virtual, 11−13 August. https://doi.org/10.2118/203662-MS.

Pathan, R., Singh, U., Joshi, A. D. et al. 2023. Automated Exploration of Economical and Safe Well Trajectories in Brown Oil and Gas Fields. *SPE Drill & Compl* **38** (4): 631–644. https://doi.org/10.2118/215829-PA.

Peshkov, G., Pavlov, M., Katterbauer, K. et al. 2023. Real-Time AI Geosteering for Horizontal Well Trajectory Optimization. Paper presented at the SPE Caspian Technical Conference and Exhibition, Baku, Azerbaijan, 21−23 November. https://doi.org/10.2118/217527-MS.

Rizkiaputra, R., Nopranda, T., Ramadhan, D. et al. 2023. Optimizing Well Trajectory Using Sequential, Hybrid Sequential, and Fully Concurrent Method Utilizing Machine Learning: A Case Study of A Tight Limestone Reservoir. Paper presented at the SPE/IATMI Asia Pacific Oil & Gas Conference and Exhibition, Jakarta, Indonesia, 10−12 October. https://doi.org/10.2118/215397-MS.

Sanghyun, L. and Stephen, K. D. 2018. Optimizing Automatic History Matching for Field Application Using Genetic Algorithm and Particle Swarm Optimization. Paper presented at the Offshore Technology Conference Asia, Kuala Lumpur, Malaysia, 20−23 March. https://doi.org/10.4043/28401-MS.

Singh, U., Pathan, R., Joshi, A. D. et al. 2024. Accelerated Design of Sidetrack and Deepening Well Trajectories. *SPE J.* **29** (4): 1862–1872. https://doi.org/10.2118/218395-PA.

Vishnumolakala, N., Kesireddy, V., Dey, S. et al. 2023. Optimizing Well Trajectory Navigation and Advanced Geo-Steering Using Deep-Reinforcement Learning. Paper presented at the SPE Annual Technical Conference and Exhibition, San Antonio, Texas, USA, 16−18 October. https://doi.org/10.2118/215011-MS.

Wan, X., Jin, L., Jiang, T. et al. 2023. Developing a High-Efficiency Method for Field-Scale Simulation of a Tight and Naturally Fractured Reservoir in the Williston Basin. Paper presented at the SPE/AAPG/SEG Unconventional Resources Technology Conference, Denver, Colorado, USA, 13−15 June. https://doi.org/10.15530/urtec-2023-3868150.

Wang, Z., Gao, D., and Liu, J. 2016. Multi-Objective Sidetracking Horizontal Well Trajectory Optimization in Cluster Wells Based on DS Algorithm. *J Pet Sci Eng* **147**: 771–778. https://doi.org/10.1016/j.petrol.2016.09.046.

Wang, L., Huang, S., Li, Z. et al. 2024. Hybrid Machine Learning Model Based on GWO and PSO Optimization for Prediction of Oilwell Cement Compressive Strength under Acidic Corrosion. *SPE J.* **29** (9): 4684–4695. https://doi.org/10.2118/221485-PA.

Wang, L., Yao, Y., Luo, X. et al. 2023. A Critical Review on Intelligent Optimization Algorithms and Surrogate Models for Conventional and Unconventional Reservoir Production Optimization. *Fuel (Lond)* **350**: 128826. https://doi.org/10.1016/j.fuel.2023.128826.

Wang, S., Zhang, Y., Khebzegga, O. et al. 2022. A Semi-Analytical Solution of the Induced Stress Change in A Layered Reservoir Based on the Stress Formulation. Paper presented at the SPE/AAPG/SEG Unconventional Resources Technology Conference, American Association of Petroleum Geologists, Houston, Texas, USA, 20−22 June. https://doi.org/10.15530/urtec-2022-3705427.

Wei, Y., Jia, A., Wang, J. et al. 2020. Semi-Analytical Modeling of Pressure-Transient Response of Multilateral Horizontal Well with Pressure Drop along Wellbore. *J Nat Gas Sci Eng* **80**: 103374. https://doi.org/10.1016/j.jngse.2020.103374.

Wu, K. and Olson, J. E. 2016. Numerical Investigation of Complex Hydraulic-Fracture Development in Naturally Fractured Reservoirs. *SPE Prod & Oper* **31** (4): 300–309. https://doi.org/10.2118/173326-PA.

Yao, J., Li, Z., Liu, L. et al. 2021. Optimization of Fracturing Parameters by Modified Variable-Length Particle-Swarm Optimization in Shale-Gas Reservoir. *SPE J.* **26** (2): 1032–1049. https://doi.org/10.2118/205023-PA.

Yildiz, T. and Deniz, O. 1998. Experimental Study on the Productivity of Complex Well Configurations. Paper presented at the SPE International Conference on Horizontal Well Technology, Calgary, Alberta, Canada, 1−4 November. https://doi.org/10.2118/50433-MS.

Yu, W., Wang, W., Zheng, S. et al. 2023. Application of a Fully Coupled Fracture-Reservoir-Wellbore Model in Shale Gas Development: Perspectives on Inter-Well Fracture Interference. Paper presented at the Asia Pacific Unconventional Resources Symposium, Brisbane, Australia, 14−15 November. https://doi.org/10.2118/217317-MS.

Zhao, G. 2013. Modeling Complex Natural Fracture Network in Heterogeneous Tight Formations Using Semi-Analytical Strategy. Paper presented at the SPE Unconventional Resources Conference Canada, Calgary, Alberta, Canada, 5−7 November. https://doi.org/10.2118/167127-MS.

Zhen, L., Xianzhi, S., Zheng, W. et al. 2024. Real-Time Prediction of Wellbore Trajectory with a Dual-Input GRU(Di-GRU) Model. Paper presented at the Offshore Technology Conference Asia, Kuala Lumpur, Malaysia, 27 February–1 March. https://doi.org/10.4043/34894-MS.

Zhu, Y. and Zhao, G. 2016. Analyzing Transient Pressure and Rate Responses of Tight Oil Reservoirs Using Comparative Numerical, Analytical and Semi-Analytical Methods. Paper presented at the SPE Asia Pacific Hydraulic Fracturing Conference, Beijing, China, 24−26 August. https://doi.org/10.2118/181866-MS.